

Supporting Information

Enhanced Stability of Immobilized Pt Nanoparticles on Carbon Nanotubes through Nitrogen Heteroatoms on Doped Carbon Supports

Wen Shi^{†‡}, Kuang-Hsu Wu[†], Junyuan Xu[†], Qiang Zhang[§], Bingsen Zhang^{*†} and Dang Sheng Su^{*†}

[†]Shenyang National Laboratory for Materials Science, Institute of Metal Research, Chinese Academy of Sciences, Shenyang 110016, China; [‡]School of Materials Science and Engineering, University of Science and Technology of China, Hefei 230026, China; [†]International Iberian Nanotechnology Laboratory, Av. Mestre Jose Veiga, 4715-330 Braga, Portugal; [§]Beijing Key Laboratory of Green Chemical Reaction Engineering and Technology, Department of Chemical Engineering, Tsinghua University, Beijing 100084, China.

* To whom correspondence should be addressed.

*E-mail: bszhang@imr.ac.cn, Tel: 86-24-83970027, Fax: 86-24-83970019;

*E-mail: dssu@imr.ac.cn, Tel: 86-24-23971577, Fax: 86-24-83970019.

Figures S1-S17; Tables S1-S3

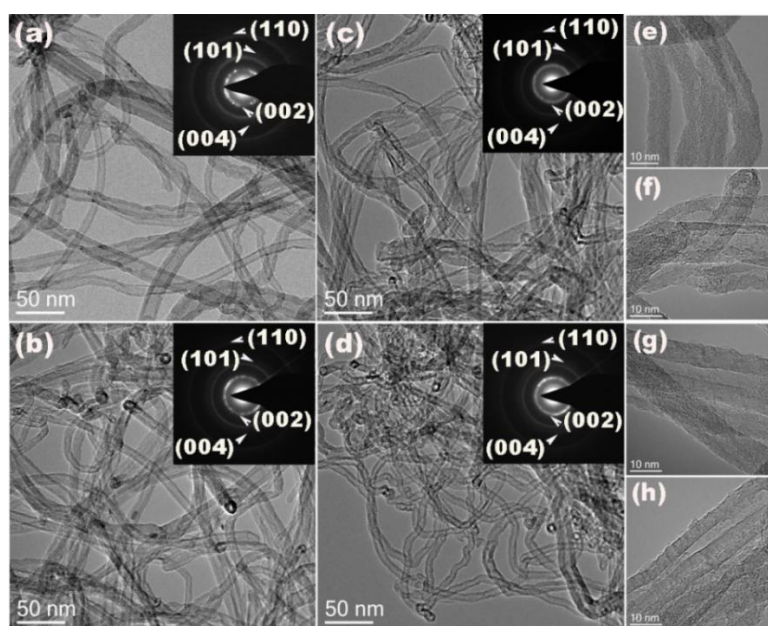


Figure S1. Low-magnification and high resolution TEM images of oCNTs (a, e), NCNTs-500 (b, f), NCNTs-700 (c, g) and NCNTs-900 (d, h). The insets are the corresponding SAED patterns.

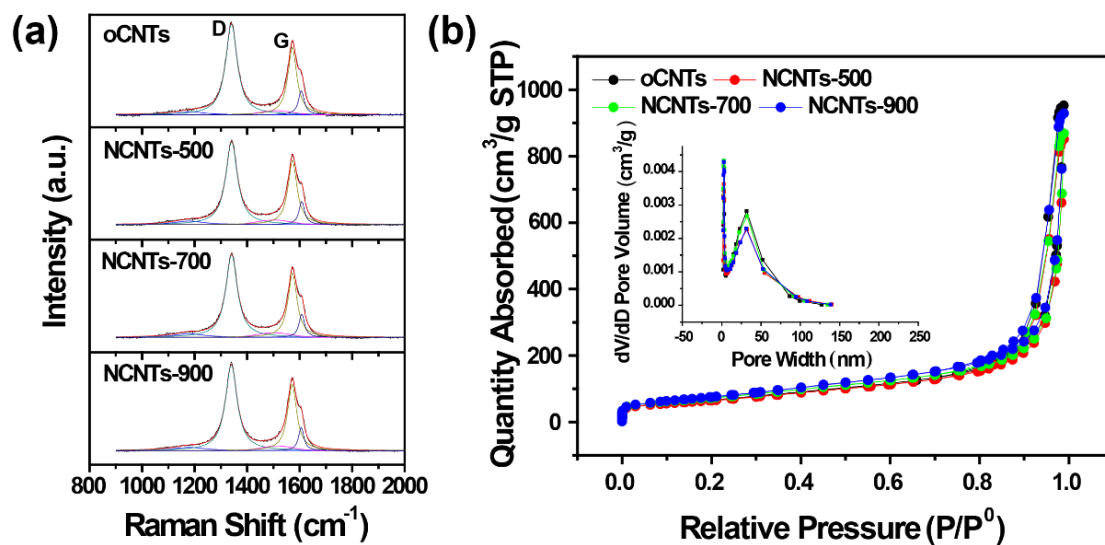


Figure S2. Raman spectra (a) and N_2 adsorption-desorption isotherms (b) of oCNTs, NCNTs-500, NCNTs-700 and NCNTs-900 samples.

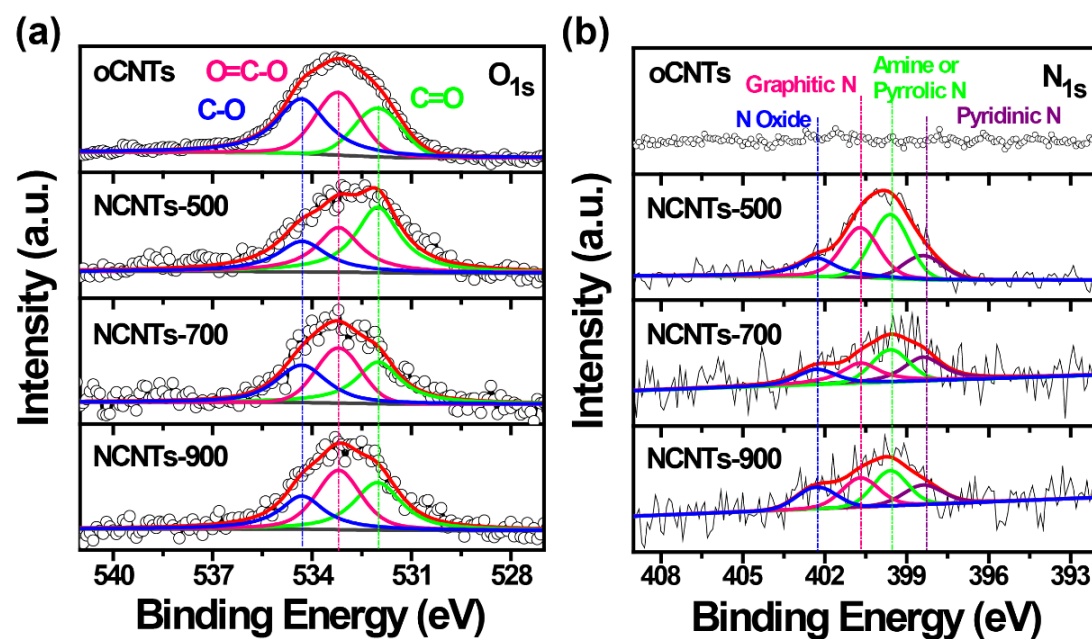


Figure S3. $\text{N } 1s$ (a) and $\text{O } 1s$ (b) spectra of oCNTs, NCNTs-500, NCNTs-700 and NCNTs-900 samples.

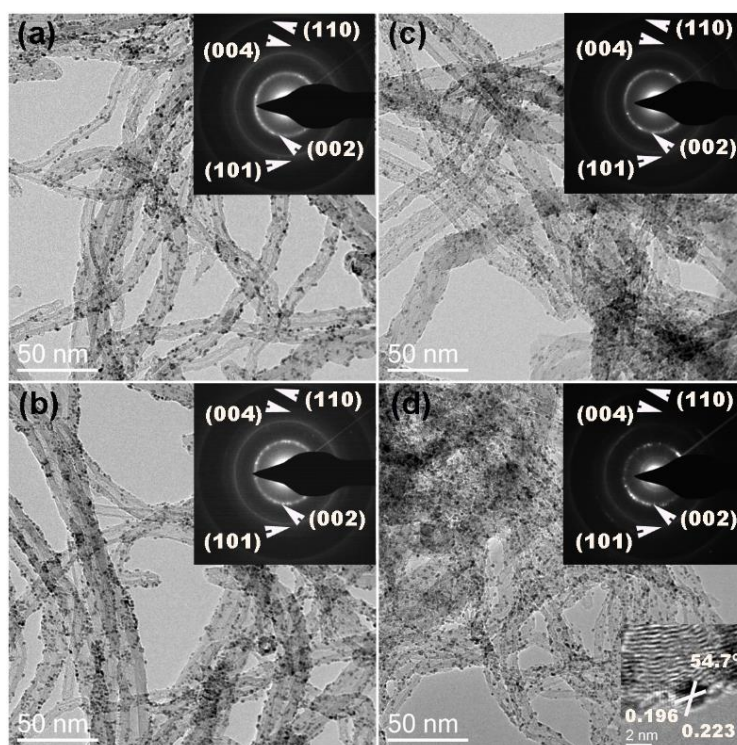


Figure S4. Low-magnification TEM images together with the corresponding SAED patterns for the Pt/oCNTs (a), Pt/NCNTs-500 (b), Pt/NCNTs-700(c) and Pt/NCNTs-900 (d) catalysts, the inset of bottom right corner in (d) is the typical HRTEM images of supported Pt NPs.

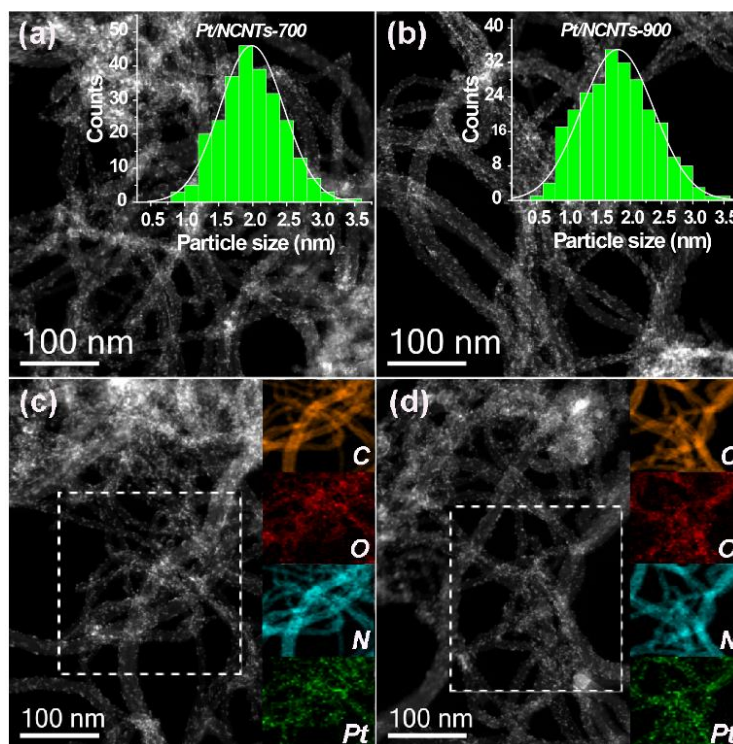


Figure S5. STEM images of Pt/NCNTs-700 (a, c) and Pt/NCNTs-900 (b, d) catalysts, the insert are the corresponding PSD and select area EDX element maps.

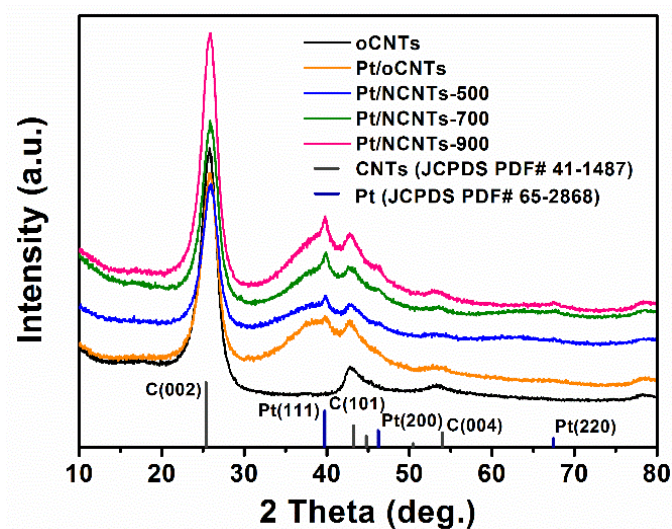


Figure S6. XRD patterns of the pristine CNTs and as-synthesized Pt based catalysts.

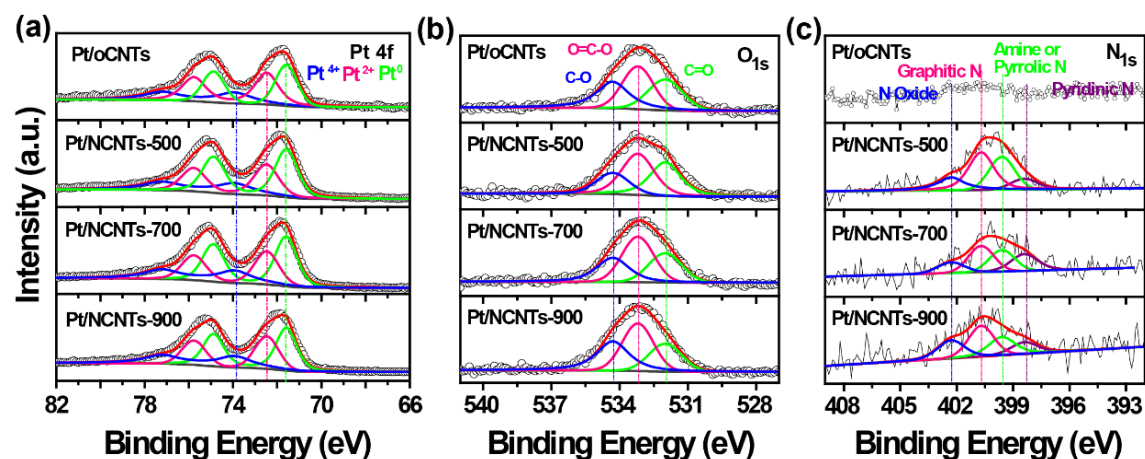


Figure S7. Pt 4f (a), N 1s (b) and O 1s (c) spectra of Pt/oCNTs, Pt/NCNTs-500, Pt/NCNTs-700, and Pt/NCNTs-900 catalysts, respectively.

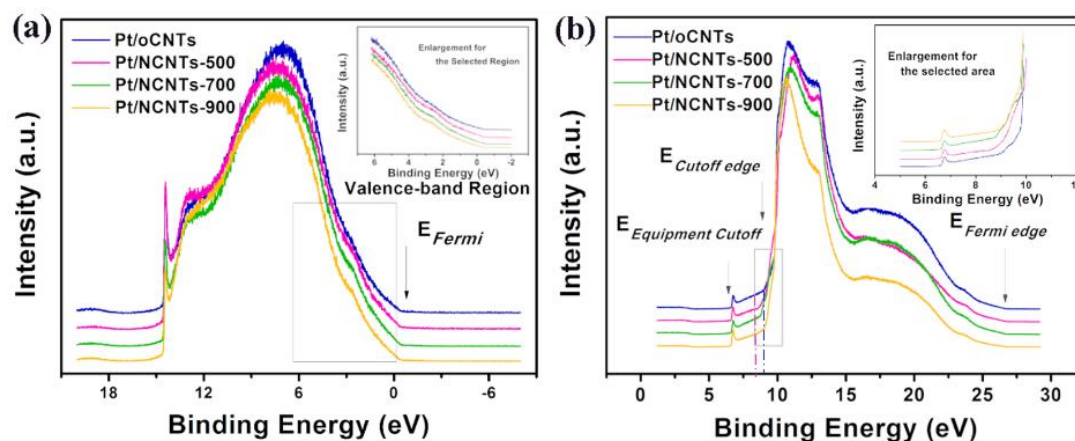


Figure S8. Valence-band spectra without (a) and with bias (b) for the prepared samples.

The deconvolution process for the XPS was referred to the method from the reported literature (Journal of American Chemical Society 2010, 132, 9616–9630). The positions and the half peak width are fixed for each species and follow certain principles. It can be seen that the fitted results match well with the originals (Figure S9). The ratio of the data from the fitted ones to the originals are all beyond 90% for Pt 4f and almost 95% for N1s, thus the corresponding error bars for the peak-fit results are below 10% and 5%, respectively. According to the detailed analysis results, it can be seen that there are some differences for the compared samples as shown in Figures 3, S3, S7 and Table S2-S3. The calculated content of Pt with zero valence state for the oCNTs and NCNTs-500 supports are 38.7% and 46.4%, respectively (Figure 3a and Table S3). With the reducing of the nitrogen content on the support, the Pt^0 component shows the regular of decreasing. That is to say that the nitrogen participation can be favorable to forming Pt with zero valence state. Accordingly, from the XPS of N1s spectra (Figure 3b and Table S3) before and after Pt loading, a decrease in the pyridinic/pyrrolic N content were observed together with an increased amount of graphitic N.

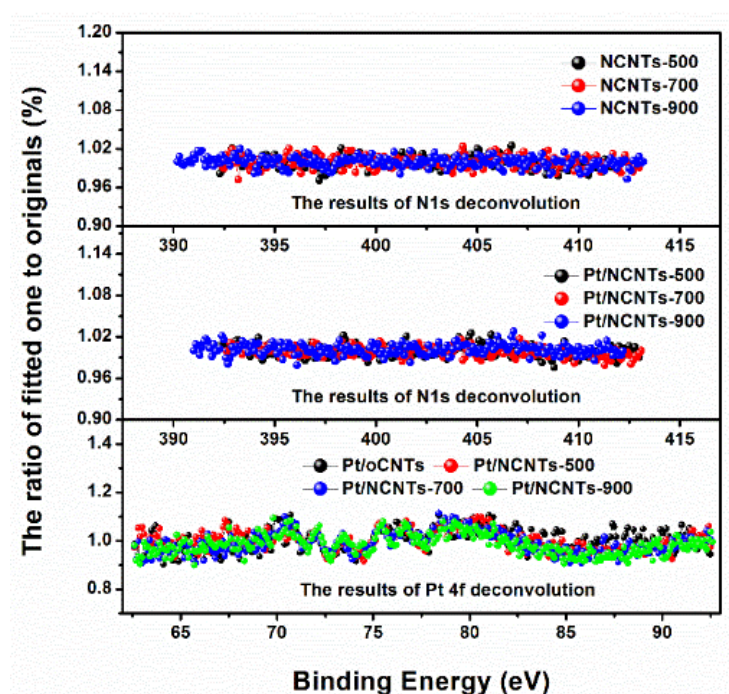


Figure S9. The ratio for the fitted data from the XPS deconvolution process and the originals.

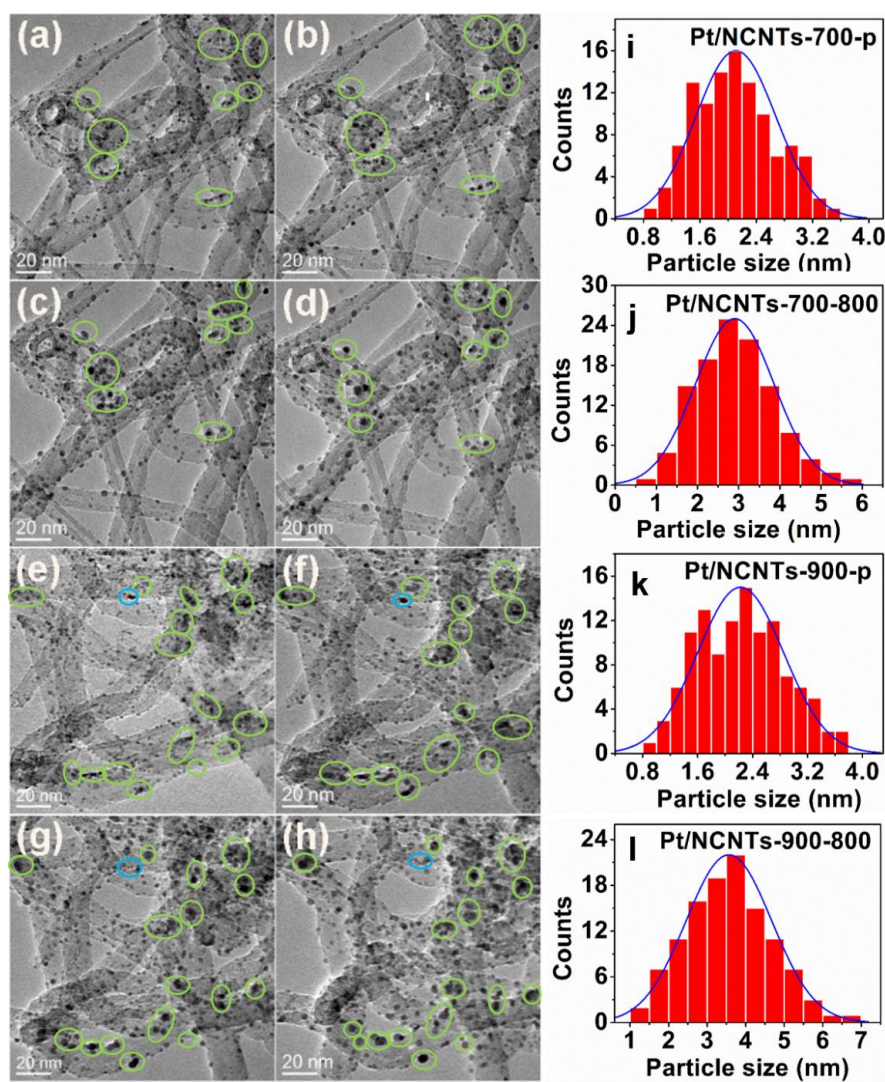


Figure S10. TEM images of Pt/NCNTs-700 (a-d) and Pt/NCNTs-900 (e-h) catalysts at temperature of 293 K (a, e), 573 K (b, f), 873 K (c, g) and 1073 K (d, h), respectively, and figures i, j, k, l are the corresponding PSD histograms.

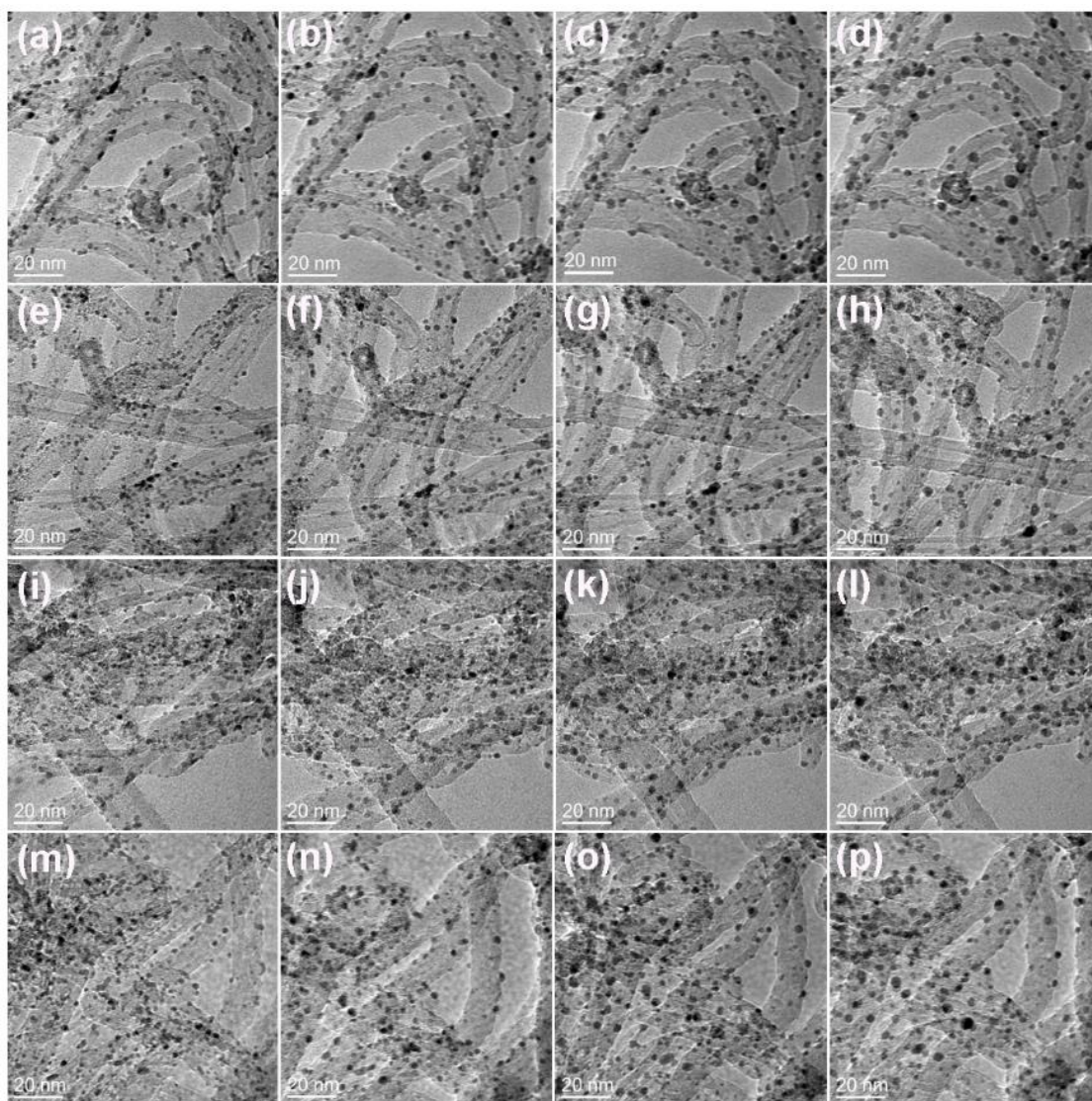


Figure S11. Low-magnification TEM images of Pt/oCNTs (a-d), Pt/NCNTs-500 (e-h), Pt/NCNTs-700 (i-l) and Pt/NCNTs-900 (m-p) catalysts at different heating temperature of 293 K (a, e, i and m), 573 K (b, f, j and n), 873 K (c, g, k and o) and 1073 K (d, h, l and p), respectively.

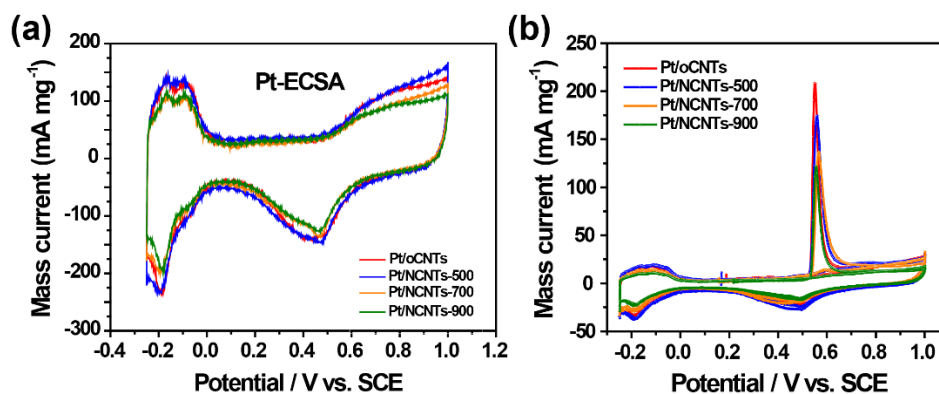


Figure S12. CV curves of the as-synthesized catalysts in 0.5 M H₂SO₄ aqueous solution (a) and CV curves of pre-absorbed CO catalysts in 0.5 M H₂SO₄ aqueous solution (b).

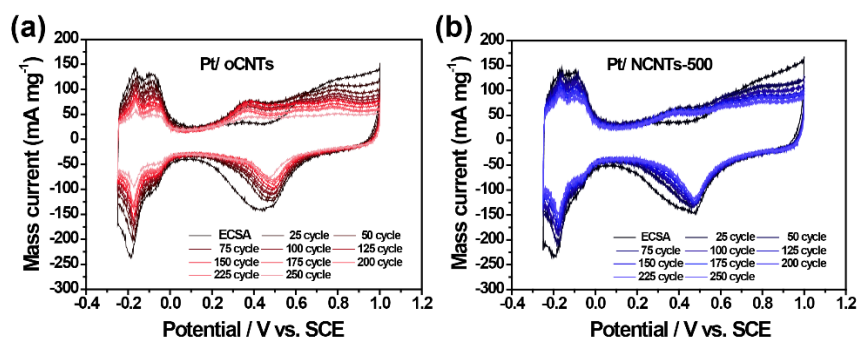


Figure S13. CV curves of the Pt/oCNTs (a) and Pt/NCNTs-500 (b) catalysts in N_2 saturated aqueous solutions of 0.5 M H_2SO_4 during the accelerated degradation tests.

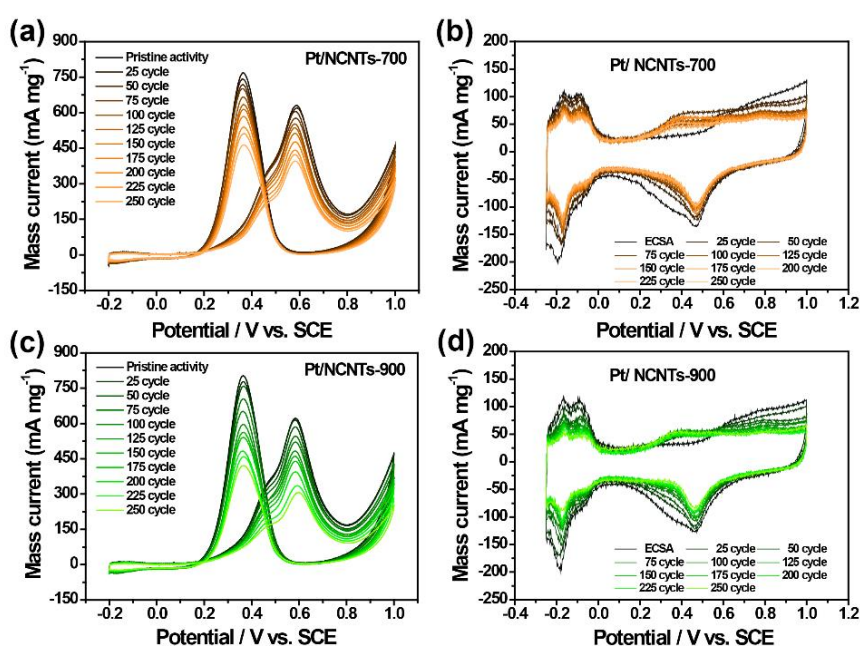


Figure S14. CV curves of the Pt/NCNTs-700 (a) and Pt/NCNTs-900 (b) catalysts in 0.5 M H_2SO_4 +0.5 M methanol aqueous solution during the accelerated degradation tests and the corresponding CV curves in N_2 saturated aqueous solutions of 0.5 M H_2SO_4 (c, d).

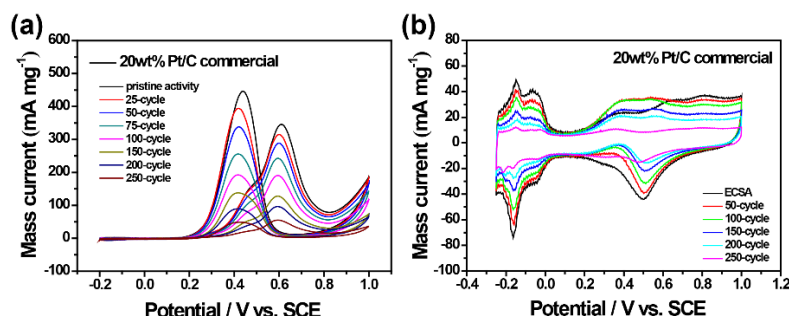


Figure S15. CV curves of the Pt/C commercial catalyst in 0.5 M H_2SO_4 +0.5 M methanol aqueous solution during the accelerated degradation test (a) and the corresponding CV curves in N_2 saturated aqueous solutions of 0.5 M H_2SO_4 (b).

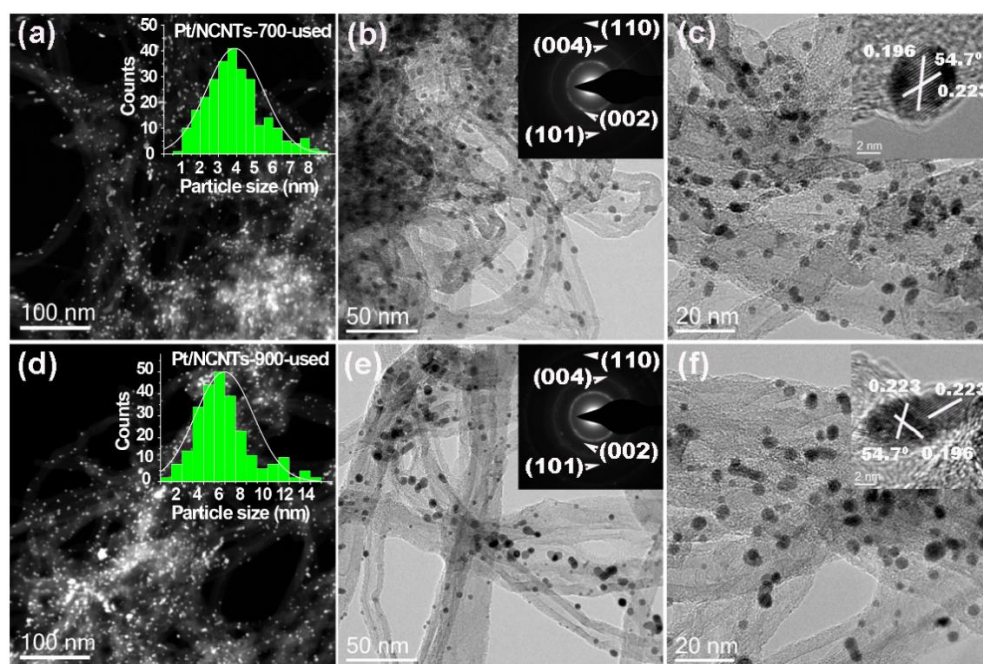


Figure S16. STEM, TEM and HRTEM images of Pt/NCNTs-700-used (a-e) and Pt/NCNTs-900-used (b-f) catalysts, the insets are the corresponding PSD histograms, SAED patterns and HRTEM images of supported Pt NPs.

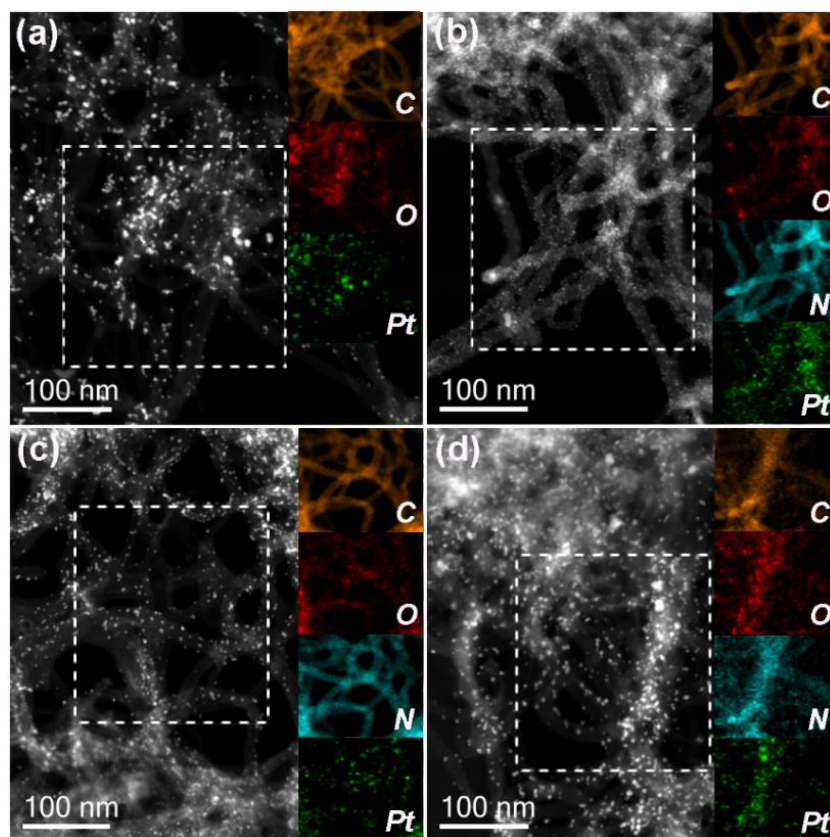


Figure S17. EDX elemental maps of Pt/oCNTs-used (a), Pt/NCNTs-500-used (b), Pt/NCNTs-700-used (c) and Pt/NCNTs-900-used (d) catalysts.

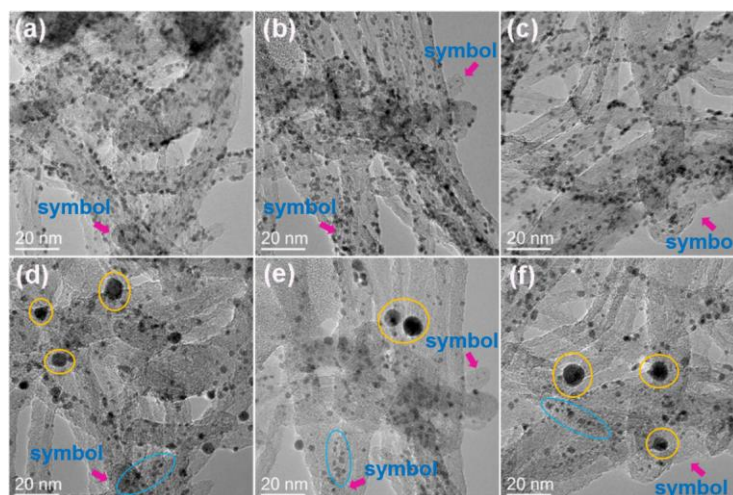


Figure S18. TEM images of Pt/oCNTs catalysts before (a-c) and after (d-f) MOR reaction at identical locations.

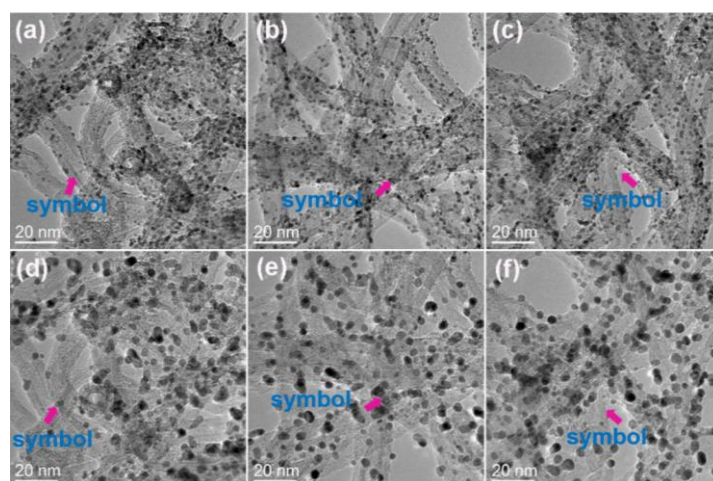


Figure S19. TEM images of Pt/NCNTs-500 catalysts before (a-c) and after (d-f) MOR reaction at identical locations.

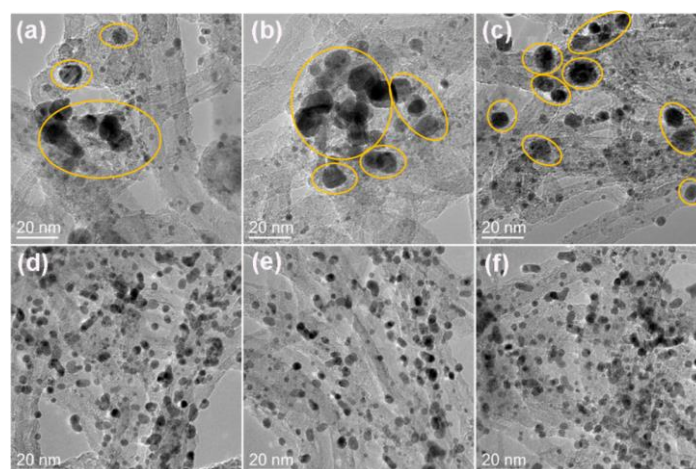


Figure S20. TEM images of Pt/oCNTs (a-c) and Pt/NCNTs-500 (d-f) catalysts at different locations after the reaction.

Table S1. The summary of Raman spectra and N₂ adsorption-desorption analysis results.

Sample	Raman	N ₂ absorption-desorption		
	I_D/I_G	S_{BET}/m^2g^{-1}	V/cm^3g^{-1}	D/nm
oCNTs	1.75	237	1.48	20.3
NCNTs-500	1.64	233	1.33	19.3
NCNTs-700	1.68	261	1.35	18.1
NCNTs-900	1.72	274	1.45	17.6

Table S2. XPS analysis of the supports and catalysts.

Sample	C at%	O at%	N at%	Pt at%
oCNTs	95.4	4.6	N/A	-
NCNTs-500	95.9	2.2	1.9	-
NCNTs-700	97.6	1.2	1.2	-
NCNTs-900	98.2	1.1	0.7	-
10 wt% Pt/oCNTs	93.6	4.5	N/A	1.9
10 wt% Pt/NCNTs-500	92.4	3.4	2.3	1.9
9.9 wt% Pt/NCNTs-700	94.1	2.9	1.2	1.8
9.2 wt% Pt/NCNTs-900	94.9	2.8	0.6	1.7

Table S3. XPS analysis of the supports and catalysts.

Sample	Pt at%			N at%				O at%		
	Pt ⁰	Pt ²⁺	Pt ⁴⁺	Pyridinic	Amine/Pyrrolic	Graphitic	N-Oxide	C=O	-O-C=O	C-O
oCNTs	-	-	-	-	-	-	-	24.6	33.3	42.1
10 wt% Pt/oCNTs	38.7	38.5	22.8	-	-	-	-	30.4	36.1	33.5
NCNTs-500	-	-	-	14.8	36.7	31.9	16.6	45.3	30.9	23.8
10 wt% Pt/NCNTs-500	46.4	32.2	21.4	10.3	29.8	41.4	18.4	36.7	42.2	21.1
NCNTs-700	-	-	-	28.3	28.6	26.6	16.5	35.2	32.7	32.1
9.9 wt% Pt/NCNTs-700	45.2	32.1	22.7	25.2	27.2	33.3	14.3	28.5	41.9	29.6
NCNTs-900	-	-	-	20.4	30.4	28.6	20.6	36.4	37.9	25.7
9.2 wt% Pt/NCNTs-900	43.4	32.9	23.7	15.6	25.2	35.3	23.9	24.7	40.2	35.1

Table S4. Comparison of ECSA, MOR activity for different catalysts.

Sample	ECSA (m ² g _{Pt} ⁻¹)	Onset oxidation potential (V)	Forward peak potential (V)	Backward peak potential (V)	I_f/I_b
10 wt% Pt/oCNTs	241.9	0.136	0.386	0.589	1.29
10 wt% Pt/NCNTs-500	234.2	0.106	0.376	0.587	1.20
9.9 wt% Pt/NCNTs-700	200.3	0.115	0.365	0.586	1.22
9.2 wt% Pt/NCNTs-900	178.2	0.139	0.362	0.584	1.28
20 wt% Pt/C	49.8	0.159	0.441	0.611	1.30